



Recovery of magnesium from flue gas desulfurization wastewater using thermomorphich hydrophilicity amines

Wenda Geng^{a,b,1}, Juncong Zou^{a,b,1}, Qiuya Niu^{a,*}, Yan Lin^a, Haiyang Liu^d, Yachao Jing^d, Chunping Yang^{a,b,c,*}

^a College of Environmental Science and Engineering, Hunan University and Key Laboratory of Environmental Biology and Pollution Control (Hunan University), Ministry of Education, Changsha, Hunan 410082, China

^b Guangdong Provincial Key Laboratory of Petrochemical Pollution Processes and Control, Key Laboratory of Petrochemical Pollution Control of Guangdong Higher Education Institutes, School of Environmental Science and Engineering, Guangdong University of Petrochemical Technology, Maoming, Guangdong 525000, China

^c School of Environmental and Chemical Engineering, Nanchang Hangkong University, Nanchang, Jiangxi 330063, China

^d Datang Environment Industry Group Co., Ltd., Beijing 100097, China

ARTICLE INFO

Keywords:

Hardness
Magnesium
Wastewater treatment
Thermomorphich hydrophilicity amine

ABSTRACT

The concentrations of hardness ions in saline wastewater from flue gas desulfurization (FGD) are usually very high, which could result in severe membrane fouling in consequent membrane systems. Hence, we investigated the feasibility of recovering Mg^{2+} from saline wastewater collected from a coal-fired power plant through utilizing thermomorphich hydrophilicity amines. Triethylamine (TEA), diisopropylamine (DIPA) and N,N-dimethylisopropylamine (DMIPA) were chosen as thermomorphich hydrophilicity amines. The effects of temperature change on solubility of amines in aqueous phase were evaluated, and the influences of molar ratio of amine to Mg^{2+} were also investigated. Results show that the solubility of amines in aqueous phase decreased substantially when temperature was increased from 25 °C to 60 °C. Thermomorphich hydrophilicity amines could be regenerated by mild heating, and regenerated TEA could remove up to 95% of Mg^{2+} in the actual FGD wastewater. Meanwhile, three amines could effectively increase the pH value of the solutions, and the recovery of Mg^{2+} was more than 98% as $Mg(OH)_2$ at an amine ratio molar ratio of 2.5. This study demonstrated the great potential of using thermoresponsive amines as alkali sources to recover Mg^{2+} and the synthesis of reactive MgO in FGD wastewater, providing a reference for the recovery of resources such as Mg^{2+} .

1. Introduction

Sulfur dioxide (SO_2) is a main air pollutant released from coal-fired power plants [1]. The limestone-gypsum process is widely applied in coal-fired power plants for the control of SO_2 emission due to its advantages of high desulfurization efficiency [2], stable operation [3] and good tolerance to different types of coals [4]. In order to protect the system from corrosion, maintain calcium sulfate crystallization rate, and keep the concentration of chloride ions in the circulating slurry under control, a portion of flue gas desulfurization (FGD) wastewater must be discharged from the system [2,5]. Generally, FGD wastewater contains a considerable amount of chloride ions, hardness ions, suspended solids and a trace number of heavy metals [6]. There are other kinds of such saline wastewater, such as reject brine [7,8], inland desalination

concentrates [9], landfill leachates [10], brines from geological carbon sequestration sites [11] and so on. Reject brine is the product from desalination processes containing high salinity, high temperature, and at many times, dissolved chemicals. These ions probably accumulate in the aquatic food chain, causing them to have a negative impact on water quality and aquatic life [12].

With the implementation of more stringent emission standards, conventional treatment and discharge of FGD wastewater cannot meet the increased environmental demands. Currently, evaporative crystallization [4,13] and membrane technology [14–17] have been widely used to handle FGD wastewater. However, the residual Ca^{2+} and Mg^{2+} in the treated FGD wastewater scale on the evaporation crystallization equipment, which reduces the heat transfer efficiency and increases the operational cost. Hence, it is necessary to remove hardness ions from

* Corresponding authors at: College of Environmental Science and Engineering, Hunan University, Changsha, Hunan 410082, China (Q.Y. Niu and C.P. Yang).
E-mail addresses: niuqiuya@hnu.edu.cn (Q. Niu), yangc@hnu.edu.cn (C. Yang).

¹ These authors contribute equally to this article.

wastewater so that the membrane system could be operated properly [18].

Conventional chemical precipitation is the effective pretreatment method for removing several scale-forming species such as Ca^{2+} and Mg^{2+} from FGD wastewater [19]. There are three steps in a typical chemical precipitation process [20]: a) neutralization and precipitation by adding alkalis (NaOH , Ca(OH)_2 , NH_4OH and other alkalis) to increase the pH and remove metal ions [20]; b) heavy metal ions removal via using metal ion trapping agents, for instance, organic sulfur [21]; c) coagulation and clarification in which particles and colloids are removed by flocculants, such as poly aluminum chloride, polyacrylamide and FeCl_3 [22]. Although the conventional pretreatment approach can remove the majority of Ca^{2+} and Mg^{2+} from FGD wastewater [5], it demands a variety of chemicals [23], leading to complicated handling process and high operating costs [24]. Meanwhile, the by-products of the treatment are normally not collected, resulting in a waste of resources [25]. Hence, searching for a cheap and efficient pretreatment technique for FGD wastewater is crucial for the future sustainable development of the coal-fired power industry.

Thermomorphous multiphase systems (TMSs) have recently appeared as an environment friendly technique with a great potential for applications. TMSs are blends of two or more liquid components with various polarities that have a miscible gap that is very sensitive to temperature [26]. The utilization of heating greatly alters the inter solubility of the solvents, and ultimately leading to the separation of the originally uniform blend to develop a binary system. Thus, temperature can be used as a trigger to switch between single-phase and dual-phase states [26]. Meanwhile, the temperature required for driving is relatively low ($40\text{--}80\text{ }^\circ\text{C}$). The thermal input can come from low-grade heat sources, for example, inexpensive industrial waste thermal and geothermal heat from shallow wells [27]. TMSs have been applied to recover homogeneous catalysts via liquid–liquid segregation at various temperatures [28,29]. Recent reports by Boo et al. [30,31] used this main notion to prove the feasibility of extracting water selectively from saline wastewater with heat-convertible polar solvents. They proposed a new technique based on the TMSs principle and named thermomorphous hydrophilicity base-induced precipitation (THBIP), which utilized recoverable amines with thermally responsive polarity to control the sedimentation of divalent cationic, ultimately removing 80% of hardness from 1.29 g/L to 0.34 g/L. The multifunctionality, the ease of operation and the wide array of suitable heat-sensitive solvents provide a chance for this technology to be widely used. Nevertheless, as far as we know, the removal of hardness ions from FGD wastewater with thermomorphous hydrophilicity amines has not been reported.

Based on these reports, we proposed that using thermomorphous hydrophilicity amines as a chemical precipitation method for the pretreatment of FGD wastewater. Specifically, thermoresponsive amines could elevate the pH of the solutions, then the hardness ions precipitated in the form of hydroxide. The amines could be regenerated from the descaled saline wastewater via utilizing the thermomorphous multiphase nature of the system, which could be reused as precipitants for Mg^{2+} ions. Meanwhile, the by-products (e.g., MgO) could be recovered and used in refractory materials [32], agriculture [33], catalyst [34] and construction industry [35]. The detail information on the process was described in the supporting information. Consequently, we proposed that the application of TMSs technology to FGD wastewater could not only reduce the risk of membrane fouling, but also provide potential economic benefits by the recovery of Mg^{2+} .

In this work, for the first time, we used the thermomorphous hydrophilicity amines for efficient descaling of FGD wastewater with high-scaling propensity and recovered a valuable by-product (MgO) from it. The technique utilized recyclable thermoresponsive amines with thermally responsive polarity to control the precipitation of mineral solids with divalent cations. The sensitivity of amines solubility in aqueous solution to temperature changes was explored with three amines, triethylamine (TEA), diisopropylamine (DIPA) and *N,N*-

Table 1

Characteristics of the FGD wastewater.

Item	pH	TDS	Ca^{2+}	Mg^{2+}	SO_4^{2-}	Cl^-
Value (mg/L)	6.71	127,392	449.65	16283.82	35339.32	12292.87

dimethylisopropylamine (DMIPA), and then the appropriate solvent for certain performance targets was determined. The potential for recovery of thermoresponsive amines was also proved with mild thermal stimulation and the reactivity of regenerated amines was evaluated. Meanwhile, the reaction kinetics, the physicochemical nature of the obtained Mg(OH)_2 and MgO were analyzed through some characterization techniques.

2. Materials and methods

2.1. Materials and chemicals

To elucidate the role of basicity and water solubility in the removal of scaling constituents. Bases with a smaller pK_b , exhibiting higher solubility at the precipitation-induction temperature, having negligible miscibility at the demixing temperature, and being safer and more environmentally friendly should be selected. Thus, Triethylamine (TEA, $\geq 99\%$), diisopropylamine (DIPA, $\geq 99\%$) and *N,N*-dimethylisopropylamine (DMIPA, 99%) were investigated for the recovery of Mg^{2+} in FGD wastewater. FGD wastewater (Table 1) was collected from a coal-fired power plant in Baoji, Shanxi Province, China. Analytical grade chemicals, comprising calcium chloride dihydrate ($\text{CaCl}_2 \cdot 2\text{H}_2\text{O}$), magnesium chloride hexahydrate ($\text{MgCl}_2 \cdot 6\text{H}_2\text{O}$) and sodium chloride (NaCl), were used to prepare for the simulated solutions. All reagents were analytical grade and purchased from Sinopharm Chemical Reagent Co. Ltd. (China). Deionized (DI) water ($18.25\text{ M}\Omega \cdot \text{cm}$) was utilized throughout the experiment.

2.2. Assessment of amine solubility in aqueous phase to temperature change

Three amines of various pK_b , TEA, DIPA and DMIPA were chosen to explore the miscibility of amines in water under low and high temperatures (T_L and T_H , correspondingly). Different quantities of TEA, DIPA and DMIPA (molar ratio of amine to water, θ , from 0.2 to 1.0 mol/L) were introduced into the reaction vial comprising deionized (DI) water at $T_L = 25\text{ }^\circ\text{C}$. The reaction vial was closely sealed, and the pH value of blends was determined after 1 h of equilibration under T_L . The mixtures in the reaction vial were then heated to $T_H = 60\text{ }^\circ\text{C}$ and the pH value of the mixtures at the was measured after further equilibrated for 1 h.

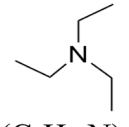
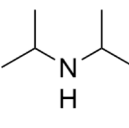
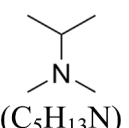
2.3. Experiments on magnesium recovery by thermosensitive amines

A simulated solution containing Mg^{2+} and Ca^{2+} (0.04 mol/L $\text{MgCl}_2 \cdot 6\text{H}_2\text{O}$, 0.013 mol/L $\text{CaCl}_2 \cdot 2\text{H}_2\text{O}$ and 2 mol/L NaCl) was used to investigate the number of mineral precipitations induced by thermoresponsive amines. Different amounts of amines were added to 100 mL of the simulated solution to explore the effects of different amine/ Mg^{2+} molar ratios (from 0.5 to 2.5) on the recovery of Mg^{2+} and Ca^{2+} . Amines were added to the solution and the preliminary pH value of the solutions was monitored. The solution was blended at a constant speed of 200 rpm in a water bath at $T_L = 25\text{ }^\circ\text{C}$. A pH probe was utilized to monitor the pH value of the solution. The experiment was terminated when the pH value of the solutions stabilized. Then the composition of the supernatant after equilibration at T_L was analyzed.

Actual FGD wastewater with high concentrations of hardness ions was also used in the study. The reaction conditions were the same as described above, and after the reaction, the solids and liquids were then separated via a centrifuge. After the precipitates were separated, they

Table 2

Chemical structure and key properties of TEA, DIPA and DMIPA.

Amine solvent	Chemical structure	Amine notes	Molecular weight [36] (g/mol)	Density*[36] (g/mL)	pK_b *[36]	Solubility in DI water*[27] (g/L)
Triethylamine (TEA)		Tertiary	101.19	0.728	2.99	133
Diisopropylamine (DIPA)		Secondary	101.19	0.722	2.95	Complete miscibility
<i>N,N</i> -dimethylisopropylamine (DMIPA)		Tertiary	87.163	0.715	3.70	Complete miscibility

*means at 25 °C.

were cleaned completely with DI water to eliminate ions adhering to the surface. The cleaning process was repeated at least three times. The washed precipitates were dried at 105 °C for 24 h. They were grounded to powder in a mortar and passed by a 125 μ m sieve, and collected to determine their physical and chemical properties. The ground samples were calcined at 500 °C and durations of 2 h within a muffle furnace to yield MgO.

2.4. Analytical methods

Mg²⁺ and Ca²⁺ concentrations in solutions were determined by atomic absorption spectrometer (AAS, PinAAcle900F, Switzerland). The pH value of the solutions was measured with a portable pH meter (PHS-3C, Leici, China). The concentrations of SO₄²⁻ and Cl⁻ were measured through an inductively coupled plasma optical emission spectrometer (ICP-OES, Agilent 725, USA). The specific surface area (SSA) of the

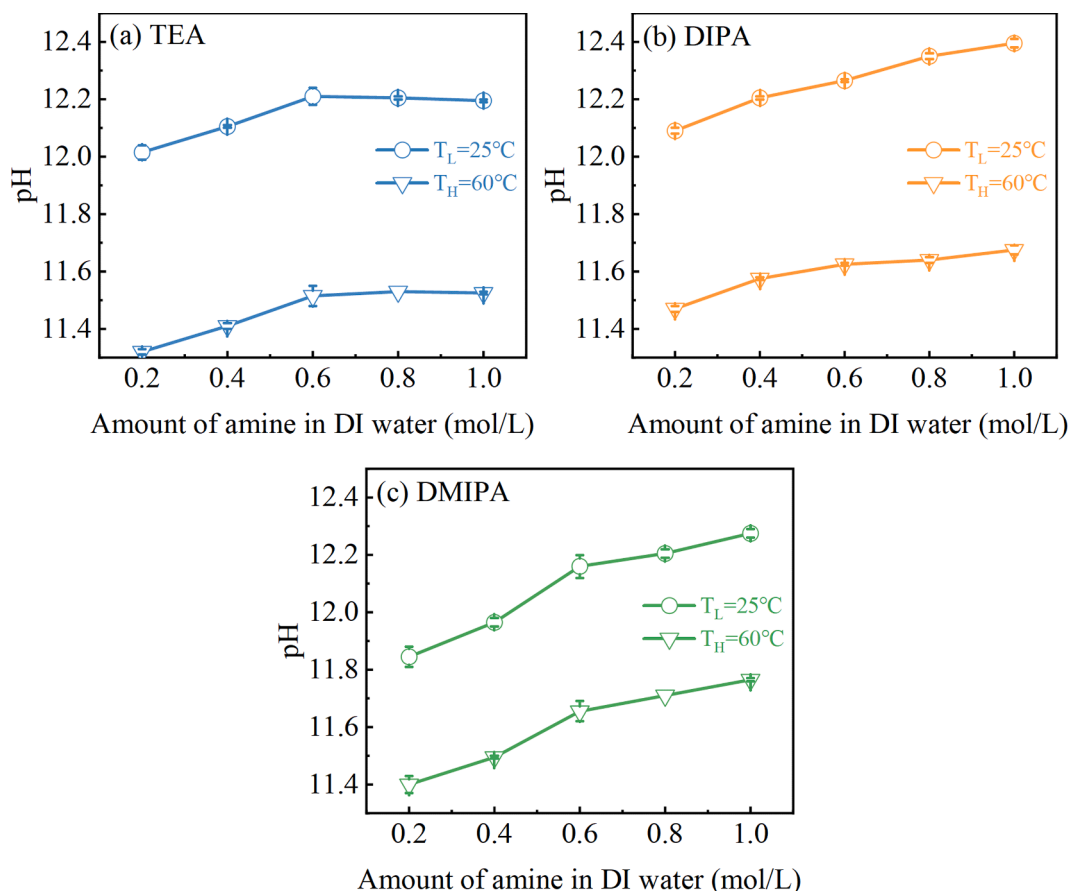


Fig. 1. Effect of different amines dosage in DI water on the pH value of the solution at $T_L = 25$ °C and $T_H = 60$ °C. (a) TEA; (b) DIPA; (c) DMIPA.

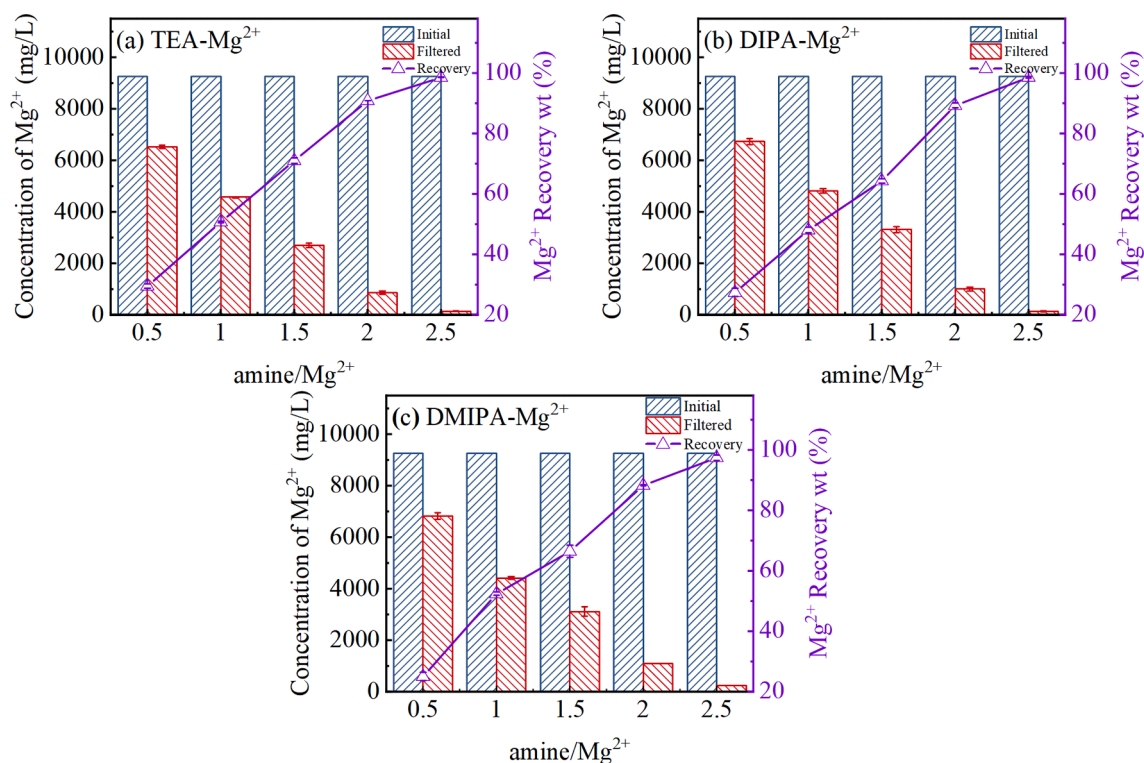


Fig. 2. Effect of amine/Mg²⁺ molar ratio of different amines on the recovery of Mg²⁺ from simulated FGD wastewater. (a) TEA; (b) DIPA; (c) DMIPA.

synthesized samples was measured by Brunauer-Emmett-Teller (BET, ASAP 2460 3.01, USA). X-ray diffraction (XRD) was detected through a D8 X-ray diffractometer (Bruker, German).

2.5. Determination of MgO reactivity

The reactivity of MgO was measured by acid neutralization, during which 0.28 g of the synthesized MgO was added into 50 mL of 0.07 mol/L citric acid solution along with phenolphthalein (i.e., pH indicator). The neutralization time from the addition of MgO to the discoloration of the solution was measured. Obviously, a shorter neutralization time means higher activity [37,38].

3. Results and discussion

3.1. Effects of amine alkalinity on descaling performance

Amines meet the basic conditions for descaling by raising the pH value of the solutions. The amine is a base and reacts with water to form hydroxide ions, i.e., $\text{amine} + \text{H}_2\text{O} \rightarrow \text{amine} - \text{H}^+ + \text{OH}^-$. Therefore, the amine is supposed to be a strong alkali and has a high solubility in water. Alkalinity can be quantitatively characterized by the dissociation constant, K_b , the thermodynamic equilibrium constant of the reaction between the amine base and the conjugate acid: $\text{amine} + \text{H}_2\text{O} \rightarrow \text{amine} - \text{H}^+ + \text{OH}^-$. K_b could be expressed by the equilibrium activity of the species in the aqueous phase: $K_b = \frac{\{\text{amine} - \text{H}^+\} \{\text{OH}^-\}}{\{\text{amine}\}}$. A larger K_b or a smaller $pK_b = -\log K_b$ indicated stronger alkalinity. To study the effects of alkalinity and miscibility of amines on the descaling performance, three amines of various pK_b and water solubility were chosen. The chemical structures and major chemical properties of triethylamine, diisopropylamine and *N,N*-dimethylisopropylamine (TEA, DIPA and DMIPA, respectively) were summarized in Table 2.

As shown in Table 2, the order of decreasing alkalinity of three amines was DIPA, TEA, and DMIPA, and their pK_b values of 2.95, 2.99 and 3.70, correspondingly. The basicity of amines in aqueous solutions

was influenced by induction and solvation effects, and depended on the extent of substitution and the size of the substituents on the nitrogen atom [36]. If there were more hydrogen atoms on the nitrogen atom of amine, the spatial site resistance was smaller, the opportunities of forming hydrogen bond with water became more and the degree of solvation was greater. Then the positive ion of the amine combined with proton was more stable and basic. The three alkyl groups on tertiary amines sterically hindered solvation of the ammonium salt and restricted stabilization of the positive charge. Hence, the secondary amine (DIPA) was a stronger base than the tertiary amines, TEA and DMIPA. The tiny variance in pK_b between the two tertiary amines might be due to the different electron donating groups [27]. Therefore, among the three amines, TEA is strongly basic but has relatively low water solubility, DMIPA is highly soluble but is a weak base, whereas DIPA features both high water solubility and basicity.

3.2. Effects of temperature change on solubility of amines in aqueous phase

The three chosen amines are thermomorphous hydrophilicity, and their miscibility with water lowers with the increase of temperature, which is ascribed to the amount of free rotation of the alkyl group grows at higher temperatures. The effect of steric hindrance is amplified, with fewer water molecules associated with nitrogen atoms, resulting in a decrease in the water solubility of the amine solvent [31,39]. The basic amines were separated from the water to obtain a diphasic water-organic blend, subsequently, the pH value of the solutions decreased accordingly. The sensitivity of amines solubility to temperature changes was assessed through the comparison of pH values at $T_L = 25^\circ\text{C}$ and $T_H = 60^\circ\text{C}$ (Fig. 1). Various quantities of TEA, DIPA and DMIPA whose moles of amine per volume of solution, θ , from 0.2 to 1.0 mol/L, were introduced to DI water at $T_L = 25^\circ\text{C}$. For all amines, the pH value of the solutions was above 11.8 at 25°C after the addition of base, and the pH increased with higher θ . Specially, the pH value of the solution of DIPA was as high as 12.40 at $\theta = 1$ mol/L.

The addition of a minimal quantity of TEA ($\theta = 0.2$ mol/L) efficiently

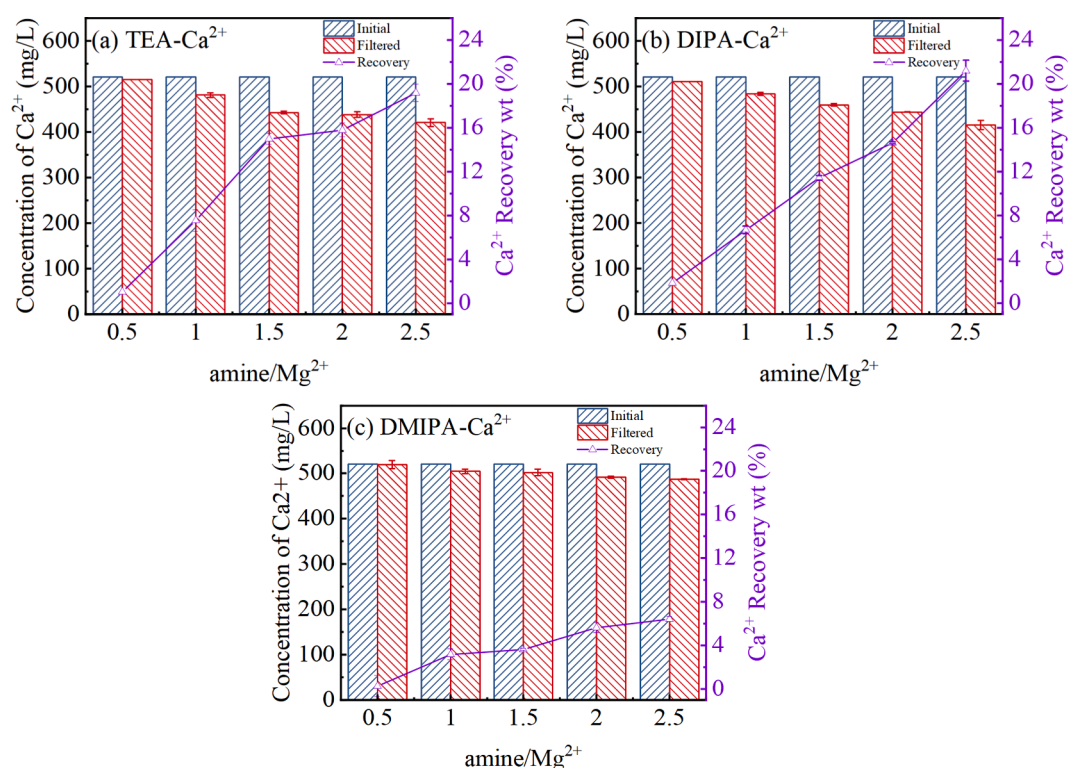


Fig. 3. Effect of amine/Mg²⁺ molar ratio of different amines on the recovery of Ca²⁺ from simulated FGD wastewater. (a) TEA; (b) DIPA; (c) DMIPA.

raised the pH value of the solutions to 12 (Fig. 1a). Nevertheless, because of the limited solubility of TEA (1.31 mol/L at 25 °C, Table 2), the introduction of TEA above $\theta = 0.6$ mol/L created an extra organic liquid layer on the top of the aqueous solution, i.e., a two-phase mixture. The pH value of the solution was effectively stabilized at ~ 12.22 , due to the incompatibility of the additional TEA with the aqueous phase (Fig. 1a). DMIPA was a weaker base than TEA (pK_b of 3.70 against 2.99, Table 2). Therefore, when $\theta = 0.2$ mol/L, the pH value of the solution was relatively lower at 11.85. However, because of the high solubility of DMIPA in the water solution, the pH value of the solution increased with the amine per solution volume over the entire study range, and the highest pH value of the solution of 12.28 was realized when θ was 1 mol/L (Fig. 1b). DIPA was a strong alkali ($pK_b = 2.95$) and had high solubility in water solution. Thus, the highest pH value of the solution increased monotonically with the increase in DIPA dosage, and the highest pH could reach 12.40 (Fig. 1c).

When the mixtures were heated to $T_H = 60$ °C, the pH value of the solution of all three amines decreased significantly. There were two reasons for the pH value of the solution drop at high temperature: the decline in $pK_a (= pK_w - pK_b)$, i.e., the basicity of the amines was low at higher temperatures, and the water solubility decreased because of the thermomorphic multiphase of the amines [26]. Boo et al. [27] have proved that an increase in temperature had an effect on pK_a and solubility, and experimentally characterized amine bases pK_a and solubility decreased in various degrees. Moreover, it could be observed through experiments that an extra organic liquid layer was generated on the top of the water solution. The upper organic liquid was carefully removed by a syringe and stored for later use. The trial outcomes confirmed the inverse correlation between the aqueous solubility of the thermoresponsive amines and temperature, and significantly, the possibility to regenerate and separate the amines via using low-grade thermal energy was demonstrated. Overall, the results highlight that warming the descaled brines using mild temperatures can trigger demixing of the thermoresponsive base from the aqueous phase, enabling the recovery of most of the amine for subsequent use. As the temperature is relatively low (60 °C in this study), the heat input can be supplied from low-grade

thermal sources, such as cheap or even free industrial waste heat, shallow-well geothermal, and low-concentration solar collectors [27].

3.3. Effects of molar ratio of amine/Mg²⁺ on recovery of Mg²⁺ from FGD wastewater

3.3.1. Simulated FGD wastewater

The recovery rate of Mg²⁺ in simulated FGD wastewater with different amounts of amines was investigated. As seen in Fig. 2, all three amines exhibited similar trends of Mg²⁺ recovery, with slight differences. The addition of a minimal quantity of amines (amine/Mg²⁺ molar ratio of 0.5) caused significant precipitation of Mg(OH)₂, and the recovery rates were 29.5%, 27.4% and 26.3% for TEA, DIPA and DMIPA, correspondingly. According to Fig. 2, the recovery rates of Mg²⁺ increased with the growth of the amine/Mg²⁺ molar ratios, which reached a resemblance to the recovery level of 94–99% of Mg²⁺ as studied in [25,40]. Therefore, practically, all Mg²⁺ ions were recovered from the solutions with the addition of enough amines.

However, the recovery of Ca²⁺ (Fig. 3) by amines was not as good as Mg²⁺, which was consistent with the results of another study [27]. The introduction of the largest amount of amine bases (amine/Mg²⁺ molar of 2.5) led to a small amount of precipitation of calcium hydroxide, and the removal rates were 19.2%, 20.3% and 6.41% for TEA, DIPA and DMIPA, respectively. It might be due to the relatively high solubility of Ca(OH)₂. The initiation of Ca(OH)₂ precipitation required a bigger pH value due to its larger K_{sp} of $10^{-5.30}$ [36]. All three amines showed a comparable trend for hardness ions removal. Introduction of the largest amount of amine bases induced massive precipitation of hardness ions, with the removal of 94.3%, 94.4% and 92.5% for TEA, DIPA and DMIPA, respectively. The measured reduction in hardness was owing to the almost complete elimination of Mg²⁺. Although DMIPA could achieve a similar recovery of Mg²⁺ as others, DMIPA was a distinctly weaker alkali than TEA and DIPA. Therefore, in order to obtain the same recovery effect as for the other investigated amines, the dosage of DMIPA was also increased accordingly. TEA had a relatively low solubility in water compared to other studied amines. But the low solubility of TEA did not

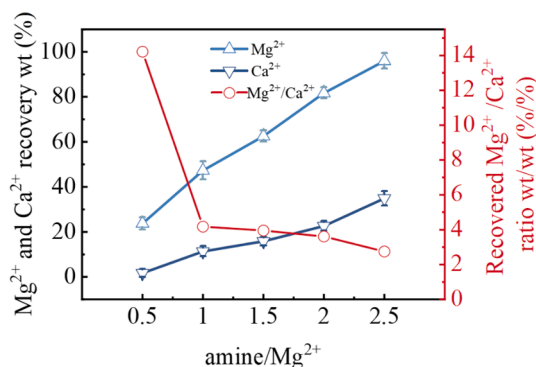


Fig. 4. Effect of amine/ Mg^{2+} molar ratio of fresh TEA on the recovery of hardness ions from actual FGD wastewater.

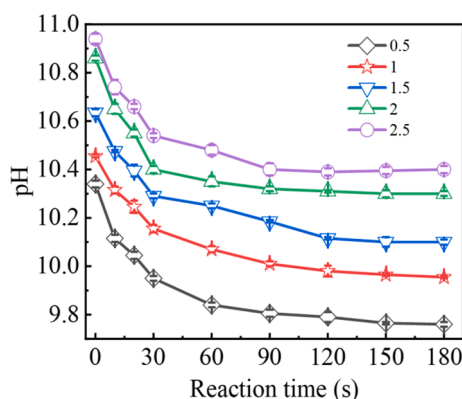


Fig. 5. Dynamic variations of pH values during the reaction between fresh TEA and actual FGD wastewater at different amine/ Mg^{2+} molar ratios.

affect the recovery of Mg^{2+} , because the dosage of TEA did not reach its solubility limit in the entire experimental range. Although DIPA was completely miscible in DI water and showed high basicity, the price of DIPA was more expensive than TEA. Therefore, TEA was selected as subsequent experiments to further evaluate the ability to recover Mg^{2+} from FGD wastewater.

3.3.2. Actual FGD wastewater

The recovery rates of hardness ions after the reaction of actual FGD wastewater with TEA were investigated. As shown in Fig. 4, the recoveries of Mg^{2+} and Ca^{2+} grew with the molar ratios of amine/ Mg^{2+} . The measured hardness reduction of 15.78 g/L at an amine molar ratio of 2.5 is owing to $\sim 95\%$ Mg^{2+} and $\sim 35\%$ Ca^{2+} removal (the initial hardness in FGD wastewater is 16.73 g/L). The sedimentation of Mg^{2+} occurred earlier than Ca^{2+} because of the K_{sp} of $\text{Mg}(\text{OH})_2$ ($10^{-11.20}$, 25 °C) [41] being lower than $\text{Ca}(\text{OH})_2$ ($10^{-5.30}$, 25 °C) [36]. Therefore, when a lower amount of TEA was used, the content of precipitated Mg^{2+} was higher than Ca^{2+} . With the addition of TEA increasing, the quantity of OH^- in solution reached the level of reaction with Ca^{2+} , thus increasing the content of $\text{Ca}(\text{OH})_2$ in the precipitates. The results demonstrated that the technology could effectively remove multivalent scale-forming ions in high-salinity brines.

The purity of the produced $\text{Mg}(\text{OH})_2$ was evaluated by the recovered $\text{Mg}^{2+}/\text{Ca}^{2+}$ ratio. According to Fig. 4, $\text{Mg}^{2+}/\text{Ca}^{2+}$ peaked at about 14.2 at the amine/ Mg^{2+} molar ratio of 0.5 and declined as molar ratio increased. It was similar to the study of Dong et al. [36,42], the $\text{Mg}^{2+}/\text{Ca}^{2+}$ ratio decreased with the increase of alkali-magnesium ratio. This might be because with the increase of amine/ Mg^{2+} ratio, that is, the increase of amine content in water, too much OH^- was provided for the reaction with Ca^{2+} . Under the circumstance, the $\text{Ca}(\text{OH})_2$ content in the precipitation increased, thus reducing the purity of the precipitation

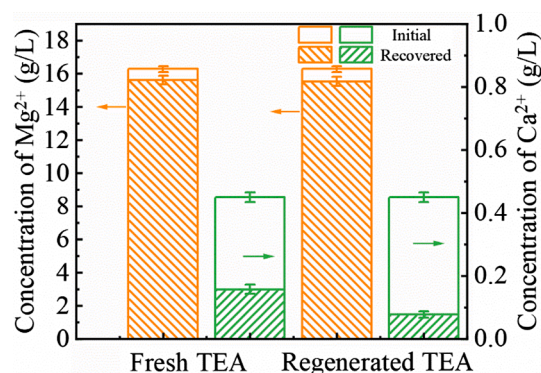


Fig. 6. Comparison of recovery of Mg^{2+} and Ca^{2+} in actual FGD wastewater by fresh TEA and regenerated TEA.

products, and the corresponding decrease of $\text{Mg}^{2+}/\text{Ca}^{2+}$ ratio. As presented in Fig. 4, although the ratio of $\text{Mg}^{2+}/\text{Ca}^{2+}$ was the largest when the amine/ Mg^{2+} is 0.5, the low dose of fresh TEA could not reach the supersaturation of $\text{Mg}(\text{OH})_2$, resulting in a lower precipitate yields. Therefore, in order to produce $\text{Mg}(\text{OH})_2$ in a large quantities, the amine/ Mg^{2+} ratio of 2 was selected for the further studies.

3.3.3. Reaction kinetics

The reaction kinetics between actual FGD wastewater and fresh amines showed by the variation of pH were concluded in Fig. 5. The reaction was finished rapidly in fewer than 180 s when the pH achieved an equilibrium state. This was in agreement with the reaction equilibrium time of the simulated wastewater studied above (Fig. S2). Both starting and ultimate pH grew with the growth of the molar ratio of amine/ Mg^{2+} . Due to the concentrations of OH^- in the solution increased, leading to quicker reaction rates and shorter reaction time [36]. It resulted in a decrease in reaction equilibrium duration from 180 s to 90 s as the amine/ Mg^{2+} molar ratios from 0.5 to 2.5, as shown in Fig. S3. Compared with other studies, the reaction equilibrium duration by using amine as an alkali source was 16.6 and 20 times shorter than utilizing NH_4OH [40] and NaOH [34] as alkali sources, respectively.

3.4. Recovery of Mg^{2+} from actual FGD wastewater with regenerated amine

Reusability is a crucial factor in evaluating the application potential of thermoresponsive amine. The amines were easily separated due to their thermoresponsive polarity and further regenerated [26]. Regenerated TEA and actual FGD wastewater were selected to evaluate the reusability of thermoresponsive amine. According to the results (Fig. 6), the initial concentrations of Mg^{2+} and Ca^{2+} in the solution were 16.28 g/L and 0.45 g/L, correspondingly. After adding regenerated TEA at amine/ Mg^{2+} of 2.5, the concentrations of Mg^{2+} and Ca^{2+} reduced to 0.75 g/L and 0.37 g/L, correspondingly (i.e., the recovery rates of Mg^{2+} and Ca^{2+} were 95% and 18%, separately). Compared to the fresh TEA, the slight decrease in recovery could be attributed to the the mixing of FGD wastewater during the recovery of TEA, which reduced the purity of regenerated TEA. In general, the removal of hardness by regenerated TEA (i.e., $\sim 93\%$) was similar to that of fresh TEA (i.e., $\sim 94\%$).

Meanwhile, the reaction kinetics between actual FGD wastewater and regenerated TEA were monitored, and the reaction equilibrium duration reached a similar level to that of the fresh TEA (Fig. 5), and the reaction reached equilibrium within 120 s (Fig. S4). Through the experimental data of the application of recovered amines to FGD wastewater for the first time, the results show that it is feasible to apply recovered amines to FGD wastewater. Compared with other studies [12,48–50], thermosensitive amines can not only be recovered, but also still have good reaction activity in FGD wastewater, which is our significant advantage.

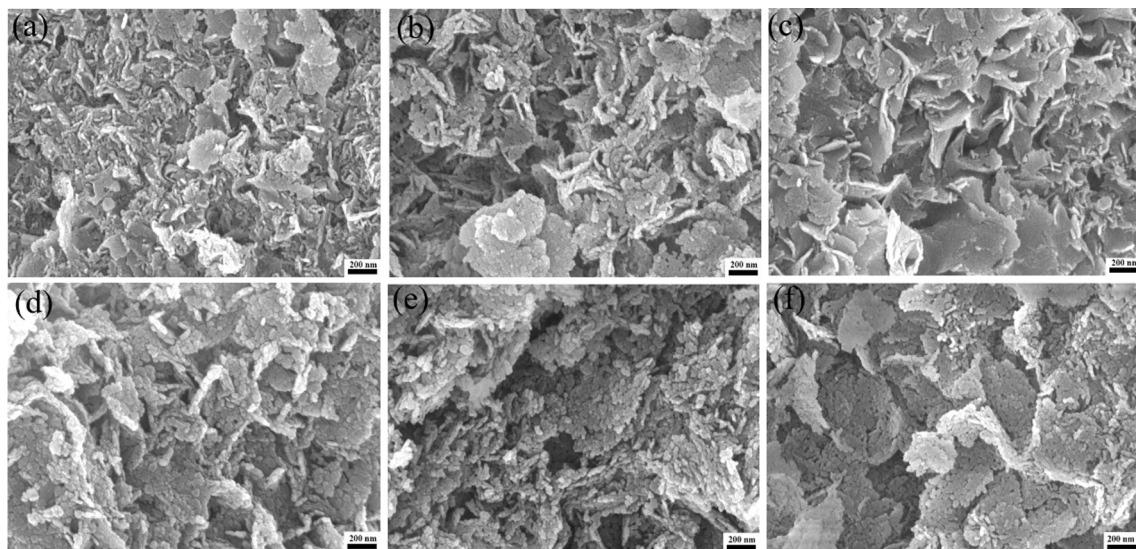


Fig. 7. SEM images of MgO were gained through calcination of $\text{Mg}(\text{OH})_2$ from the reaction of actual FGD wastewater with TEA under various amine/ Mg^{2+} molar ratios. (a) 0.5; (b) 1; (c) 1.5; (d) 2; (e-f) 2.5.

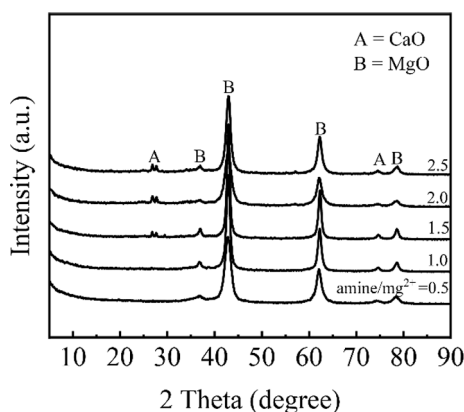


Fig. 8. XRD diffractograms of activated MgO were yielded through calcination $\text{Mg}(\text{OH})_2$ from the reaction of actual FGD wastewater with TEA at different amine/ Mg^{2+} molar ratios.

3.5. Characterization of MgO

3.5.1. SEM

Some studies investigated the effect of coating conditions on the reactivity of MgO, and they found that the increase of roasting temperature (500 °C to 700 °C) and roasting time (2 h to 12 h) would decrease the reactivity of MgO [37,43]. Thus, we chose 500 °C and 2 h as the conditions for roasting MgO in this study. The morphology of MgO yielded by calcining $\text{Mg}(\text{OH})_2$ of various amine/ Mg^{2+} molar ratios at 500 °C for 2 h was studied. As seen in Fig. 7, the morphology of MgO changed from a plate-like to a granular pattern. And the structure became more and more dense as the amine/ Mg^{2+} ratios grew. It might be related to the morphology of parent material $\text{Mg}(\text{OH})_2$ [43,44]. As the amine/ Mg^{2+} molar ratio increased, the pH value of the solutions grew. The incremental concentration of OH^- hastened the nucleation of $\text{Mg}(\text{OH})_2$ crystals and caused the formation of significant quantities of $\text{Mg}(\text{OH})_2$, which promoting the densification of the whole structure [37]. MgO exhibited a more porous structure because of the closely packed structure of $\text{Mg}(\text{OH})_2$. This finding was shown to be consistent with former researches [38,45]. The morphology of regenerated TEA-synthesized reactive MgO also was a dense granular pattern as shown in Fig. S5.

3.5.2. XRD

The XRD diffractograms of MgO gained through calcining $\text{Mg}(\text{OH})_2$ produced under various amine/ Mg^{2+} molar ratios were studied. According to Fig. 8, the main peak positions of the synthesized reactive MgO matched well with the reference peaks of MgO (JCPDS # 89-7746) with few minor peaks attributed to the presence of calcium oxide, which may have formed from the transformation of slaked lime at higher temperatures [51]. The absence of $\text{Mg}(\text{OH})_2$ peak suggested that the brucite was completely disintegrated to active MgO under the calcination conditions used in this research. The XRD diffractogram of the regenerated TEA produced by calcining $\text{Mg}(\text{OH})_2$ at the amine/ Mg^{2+} molar ratio of 2.5 showed a similar trend (Fig. S6).

3.5.3. SSA

The SSA of the activated MgO gained from FGD wastewater were compared with MgO samples mentioned in other studies [37,42,43,46]. As seen in Table 3, the SSA of the synthesized activated MgO achieved 96.9 m^2/g . It was obviously higher than that of other researches under the same conditions. For example, the SSA of synthesized MgO from chloride solution through adding NaOH was 22.1 m^2/g [46]. The main impurity (such as CaO) in the MgO samples were obtained by roasting magnesite, which leads to lower SSA. The differences in SSA values with the addition of different alkali sources may be because of the difference in the properties of the precursor, $\text{Mg}(\text{OH})_2$ (i.e., amine-based $\text{Mg}(\text{OH})_2$ possessed a higher SSA and porosity than NH_4OH -based and NaOH-based $\text{Mg}(\text{OH})_2$). This was attributed to both the influences of pH and cation structure in solutions [35]. The utilization of NaOH or NH_4OH as the base was discovered to form $\text{Mg}(\text{OH})_2$ with a spherical cauliflower-like morphology, which made the MgO sample higher agglomeration ratio [37,42]. While amines were used as the base source, the calcined MgO samples had a more porous structure, which led to a higher SSA value. According to the categorization of MgO suggested by Jin et al [47], the gained MgO in this research can be categorized as “category I”, which refers to highly reactive MgO with a SSA of over 60 m^2/g . The SSA can be further improved by optimizing production conditions.

3.5.4. Reactivity

The comparison between the reactivity and SSA of MgO were shown in Table 3, where a negative correlation between these two parameters was found. Accordingly, MgO samples with higher SSA brought about shorter acid neutralization times, which indicated their higher reactivity. These results were consistent with those reported in other studies

Table 3
Properties of reactive MgO from different sources.

Base/Name	Source	SSA (m ² /g)	Reactivity (s)	Category	Reference
94/200	Magnesite	4.37	976	III	[47]
NaOH	Synthetic solution	22.1	–	II	[46]
NH ₄ OH	Reject saline wastewater	78.8	–	I	[42]
NaOH	Reject saline wastewater	51.4	664	II	[37]
Amine (TEA)	FGD wastewater	96.9	397	I	This work
Regenerated amine (TEA)	FGD wastewater	71.4	375	I	This work

[38,43,47]. Meanwhile, it is found that the data of the SSA (71.4 m²/g) and acid neutralization time (375 s) of the MgO calcined by the regenerated amine presented in Table 3 indicated that the regenerated amine still showed good reactivity. The properties of high SSA and reactivity of MgO obtained in this study provide a wide range of potential applications for MgO. Meanwhile, this study demonstrated that FGD wastewater can be considered as a feasible and economic alternative source for the sustainable recovery of MgO with a high reactivity.

4. Conclusions

In this study, thermosensitive amines were used as alkali source to recover magnesium from FGD wastewater, and the properties of the recovered product were studied. TEA, DMIPA and DIPA were all effective in raising the pH of FGD wastewater, resulting in Mg²⁺ removal rates of more than 98%. The Mg²⁺ in actual FGD wastewater could remove up to ~95% by the addition of fresh TEA. The synthesized Mg(OH)₂ was calcined at 500 °C for 2 h to obtain highly active MgO with a SSA of 96.94 m²/g. The regenerated amine showed excellent reusability (recovering 96% of Mg²⁺ from FGD wastewater) and simultaneously obtained MgO with a SSA of 71.40 m²/g. The features of amine recyclability and low-grade heat utilization can potentially enable it to be a cost-effective technology for descaling hypersaline brines. This technology can not only realize the zero liquid discharge of FGD wastewater, but also recover by-products for resource utilization and promote the sustainable development of the power industry.

CRediT authorship contribution statement

Wenda Geng: Investigation, Conceptualization, Methodology, Writing – original draft. **Juncong Zou:** Conceptualization, Methodology. **Qiuya Niu:** Writing – review & editing, Supervision. **Yan Lin:** Funding acquisition, Writing – review & editing. **Haiyang Liu:** Conceptualization, Methodology. **Yachao Jing:** Conceptualization, Methodology. **Chunping Yang:** Funding acquisition, Writing – review & editing.

Declaration of Competing Interest

The authors declare that they have no known competing financial interests or personal relationships that could have appeared to influence the work reported in this paper.

Data availability

Data will be made available on request.

Acknowledgments

This work was supported by the National Natural Science Foundation of China (Grant No.: 51978178 and 51521006), the Department of Science and Technology of Guangdong Province of China (Contract No.: 2019A1515012044), Maoming Municipal Department of Science and Technology of Guangdong Province of China (Contract No.: 2018S0013), the Key Laboratory of Petrochemical Pollution Control of

Guangdong Higher Education Institutes (KLGHEI 2017KSYS004), China Postdoctoral Science Foundation (No.: 2021M701150), the Science and Technology Innovation Program of Hunan Province of China (Contract No.: 2021RC2058).

Appendix A. Supplementary data

Supplementary data to this article can be found online at <https://doi.org/10.1016/j.seppur.2023.123776>.

References

- [1] Z. Zhu, Y. Ma, Z. Qu, L. Fang, W. Zhang, N. Yan, Study on a new wet flue gas desulfurization method based on the Bunsen reaction of sulfur-iodine thermochemical cycle, *Fuel* 195 (2017) 33–37, <https://doi.org/10.1016/j.fuel.2017.01.045>.
- [2] C. Xu, J. Hong, Y. Ren, Q. Wang, X. Yuan, Approaches for controlling air pollutants and their environmental impacts generated from coal-based electricity generation in China, *Environ. Sci. Pollut. Res.* 22 (2015) 12384–12395, <https://doi.org/10.1007/s11356-015-4539-y>.
- [3] C. Zheng, H. Zheng, Z. Yang, S. Liu, X. Li, Y. Zhang, W. Weng, X. Gao, Experimental study on the evaporation and chlorine migration of desulfurization wastewater in flue gas, *Environ. Sci. Pollut. Res.* 26 (2019) 4791–4800, <https://doi.org/10.1007/s11356-018-3816-y>.
- [4] H. Zheng, C. Zheng, X. Li, S. Xu, S. Liu, Y. Zhang, W. Weng, X. Gao, Evaporation and concentration of desulfurization wastewater with waste heat from coal-fired power plants, *Environ. Sci. Pollut. Res.* 26 (2019) 27494–27504, <https://doi.org/10.1007/s11356-019-05297-6>.
- [5] S. Ma, J. Chai, K. Wu, Y. Xiang, S. Jia, Q. Li, Experimental research on bypass evaporation tower technology for zero liquid discharge of desulfurization wastewater, *Environ. Technol.* 40 (2019) 2715–2725, <https://doi.org/10.1080/09593330.2018.1449901>.
- [6] Z. Liang, L. Zhang, Z. Yang, T. Qiang, G. Pu, J. Ran, Evaporation and crystallization of a droplet of desulfurization wastewater with waste heat from coal-fired power plant, *Appl. Therm. Eng.* 119 (2017) 52–62, <https://doi.org/10.1016/j.applthermaleng.2017.02.113>.
- [7] A. Giwa, V. Dufour, F. Al Marzooqi, M. Al Kaabi, S.W. Hasan, Brine management methods: Recent innovations and current status, *Desalination* 407 (2017) 1–23, <https://doi.org/10.1016/j.desal.2016.12.008>.
- [8] J.C. Zou, Y. Lin, S.H. Wu, M.J. Wu, C.P. Yang, Construction of bifunctional 3-D ordered mesoporous catalyst for oxidative desulfurization, *Sep. Purif. Technol.* 264 (2021), 118434, <https://doi.org/10.1016/j.seppur.2021.118434>.
- [9] P.V. Brady, R.J. Kottenstette, T.M. Mayer, M.M. Hightower, Inland Desalination: Challenges and Research Needs, *J. Contemp. Wat. Res. Ed* 132 (2009) 46–51, <https://doi.org/10.1111/j.1936-704X.2005.mp132001007.x>.
- [10] Z. Salem, K. Hamouri, R. Djemaa, K. Allia, Evaluation of landfill leachate pollution and treatment, *Desalination* 220 (2008) 108–114, <https://doi.org/10.1016/j.desal.2007.01.026>.
- [11] J.T. Arena, J.C. Jain, C.L. Lopano, J.A. Hakala, T.V. Bartholomew, M.S. Mauter, N. S. Siefert, Management and dewatering of brines extracted from geologic carbon storage sites, *Int. J. Greenh. Gas. Con* 63 (2017) 194–214, <https://doi.org/10.1016/j.jggc.2017.03.032>.
- [12] X. Zhang, C. Ye, K. Pi, J. Huang, M. Xia, A.R. Gerson, Sustainable treatment of desulfurization wastewater by ion exchange and bipolar membrane electrodialysis hybrid technology, *Sep. Purif. Technol.* 211 (2019) 330–339, <https://doi.org/10.1016/j.seppur.2018.10.003>.
- [13] A.B. Schantz, B. Xiong, E. Dees, D.R. Moore, X. Yang, M. Kumar, Emerging investigators series: prospects and challenges for high-pressure reverse osmosis in minimizing concentrated waste streams, *Environ. Sci.-Wat. Res.* 4 (2018) 894–908, <https://doi.org/10.1039/c8ew00137e>.
- [14] L. Cui, Y. Li, Y. Tang, Y. Shi, Q. Wang, X. Yuan, J. Kellett, Integrated assessment of the environmental and economic effects of an ultra-clean flue gas treatment process in coal-fired power plant, *J. Clean. Prod.* 199 (2018) 359–368, <https://doi.org/10.1016/j.jclepro.2018.07.174>.
- [15] O. Alrehaili, F. Perreault, S. Sinha, P. Westerhoff, Increasing net water recovery of reverse osmosis with membrane distillation using natural thermal differentials between brine and co-located water sources: Impacts at large reclamation facilities, *Water Res.* 184 (2020), 116134, <https://doi.org/10.1016/j.watres.2020.116134>.

- [16] G. Guan, H. Lou, C. Yao, J. Li, X. Yang, Achieving sustainable operation for hypersaline membrane distillation applications: A novel strategy based on the critical Reynolds number, *Desalination* 499 (2021), 114833, <https://doi.org/10.1016/j.desal.2020.114833>.
- [17] J.C. Zou, Y. Lin, C.P. Yang, Covalency triggers high catalytic activity of amorphous molybdenum oxides for oxidative desulfurization, *Sci. China-Chem.* 66 (2023) 1211–1220, <https://doi.org/10.1007/s11426-022-1534-8>.
- [18] Y. Huang, P.K. Peddi, C. Tang, H. Zeng, X. Teng, Hybrid zero-valent iron process for removing heavy metals and nitrate from flue-gas-desulfurization wastewater, *Sep. Purif. Technol.* 118 (2013) 690–698, <https://doi.org/10.1016/j.seppur.2013.07.009>.
- [19] Q. Cheng, Y. Wu, Y. Huang, F. Li, Z. Liu, L. Nengzi, L. Bao, An integrated process of calcium hydroxide precipitation and air stripping for pretreatment of flue gas desulfurization wastewater towards zero liquid discharge, *J. Clean. Prod.* 314 (2021), 128077, <https://doi.org/10.1016/j.jclepro.2021.128077>.
- [20] J. Yan, W. Yuan, J. Liu, W. Ye, J. Lin, J. Xie, X. Huang, S. Gao, J. Xie, S. Liu, W. Chen, H. Zhang, An integrated process of chemical precipitation and sulfate reduction for treatment of flue gas desulfurization wastewater from coal-fired power plant, *J. Clean. Prod.* 228 (2019) 63–72, <https://doi.org/10.1016/j.jclepro.2019.04.227>.
- [21] P. Córdoba, Status of Flue Gas Desulfurization (FGD) systems from coal-fired power plants: Overview of the physico-chemical control processes of wet limestone FGDs, *Fuel* 144 (2015) 274–286, <https://doi.org/10.1016/j.fuel.2014.12.065>.
- [22] J. Shi, Y. Dang, D. Qu, D. Sun, Effective treatment of reverse osmosis concentrate from incineration leachate using direct contact membrane distillation coupled with a NaOH/PAM pre-treatment process, *Chemosphere* 220 (2019) 195–203, <https://doi.org/10.1016/j.chemosphere.2018.12.110>.
- [23] S. Lee, Y. Kim, S. Hong, Treatment of industrial wastewater produced by desulfurization process in a coal-fired power plant via FO-MD hybrid process, *Chemosphere* 210 (2018) 44–51, <https://doi.org/10.1016/j.chemosphere.2018.06.180>.
- [24] D.B. Gingerich, E. Grol, M.S. Mauter, Fundamental challenges and engineering opportunities in flue gas desulfurization wastewater treatment at coal fired power plants, *Environ. Sci.-Wat. Res. Technol.* 4 (2018) 909–925, <https://doi.org/10.1039/c8ew00264a>.
- [25] S. Ma, J. Chai, G. Chen, W. Yu, S. Zhu, Research on desulfurization wastewater evaporation: Present and future perspectives, *Renew. Sust. Energ. Rev.* 58 (2016) 1143–1151, <https://doi.org/10.1016/j.rser.2015.12.252>.
- [26] J. Bianga, K.U. Kunnemann, T. Gaide, A.J. Vorholt, T. Seidensticker, J. M. Dreimann, D. Vogt, Thermomorphic multiphase systems: switchable solvent mixtures for the recovery of homogeneous catalysts in batch and flow processes, *Chemistry* 25 (2019) 11586–11608, <https://doi.org/10.1002/chem.201902154>.
- [27] C. Boo, H. Qi, I.H. Billinge, K.M. Shah, H. Fan, N.Y. Yip, Thermomorphic hydrophilicity base-induced precipitation for effective descaling of hypersaline brines, *ACS ES&T Eng.* 1 (2021) 1351–1359, <https://doi.org/10.1021/acsestengg.1c00160>.
- [28] G. Kiedorf, D.M. Hoang, A. Müller, A. Jörke, J. Markert, H. Arellano-Garcia, A. Seidel-Morgenstern, C. Hamel, Kinetics of 1-dodecene hydroformylation in a thermomorphic solvent system using a rhodium-biphenyl catalyst, *Chem. Eng. Sci.* 115 (2014) 31–48, <https://doi.org/10.1016/j.ces.2013.06.027>.
- [29] K. McBride, T. Gaide, A. Vorholt, A. Behr, K. Sundmacher, Thermomorphic solvent selection for homogeneous catalyst recovery based on COSMO-RS, *Chem. Eng. Process.* 99 (2016) 97–106, <https://doi.org/10.1016/j.ces.2015.07.004>.
- [30] C. Boo, I.H. Billinge, X. Chen, K.M. Shah, N.Y. Yip, Zero liquid discharge of ultrahigh-salinity brines with temperature swing solvent extraction, *Environ. Sci. Technol.* 54 (2020) 9124–9131, <https://doi.org/10.1021/acs.est.0c02555>.
- [31] C. Boo, R.K. Winton, K.M. Conway, N.Y. Yip, Membrane-less and non-evaporative desalination of hypersaline brines by temperature swing solvent extraction, *Environ. Sci. Technol. Lett.* 6 (2019) 359–364, <https://doi.org/10.1021/acs.estlett.9b00182>.
- [32] M.A. Faghihi-Sani, A. Yamaguchi, Oxidation kinetics of MgO–C refractory bricks, *Ceram. Int.* 28 (2002) 835–839, [https://doi.org/10.1016/S0272-8842\(02\)00049-4](https://doi.org/10.1016/S0272-8842(02)00049-4).
- [33] A.A. Pilarska, L. Klapiszewski, T. Jesionowski, Recent development in the synthesis, modification and application of Mg(OH)₂ and MgO: A review, *Powder Technol.* 319 (2017) 373–407, <https://doi.org/10.1016/j.powtec.2017.07.009>.
- [34] N.F. Dummer, L. Joyce, H. Ellicott, Y. Jiang, Surfactant controlled magnesium oxide synthesis for base catalysis, *Catal. Sci. Technol.* 6 (2016) 1903–1912, <https://doi.org/10.1039/c5cy01107h>.
- [35] L. Mo, M. Deng, M. Tang, A. Al-Tabbaa, MgO expansive cement and concrete in China: Past, present and future, *Cem. Concr. Res.* 57 (2014) 1–12, <https://doi.org/10.1016/j.cemconres.2013.12.007>.
- [36] H. Dong, C. Unluer, E.-H. Yang, A. Al-Tabbaa, Recovery of reactive MgO from reject brine via the addition of NaOH, *Desalination* 429 (2018) 88–95, <https://doi.org/10.1016/j.desal.2017.12.021>.
- [37] L. Mo, M. Deng, M. Tang, Effects of calcination condition on expansion property of MgO-type expansive agent used in cement-based materials, *Cem. Concr. Res.* 40 (2010) 437–446, <https://doi.org/10.1016/j.cemconres.2009.09.025>.
- [38] W.M. Haynes, *CRC Handbook of chemistry and physics*, 97th ed., CRC Press, 2014.
- [39] R.R. Davidson, W.H. Smith, D.W. Hood, Structure and amine-water solubility in desalination by solvent extraction, *J. Chem. Eng.* (1960), <https://doi.org/10.1021/je60008a005>.
- [40] S. Casas, C. Aladjem, E. Larrotcha, O. Gibert, C. Valderrama, J.L. Cortina, Valorisation of Ca and Mg by-products from mining and seawater desalination brines for water treatment applications, *J. Chem. Technol. Biotechnol.* 89 (2014) 872–883, <https://doi.org/10.1002/jctb.4326>.
- [41] G.R. Lenz, A.E. Martell, Metal complexes of carnosine, *Biochemistry* (1964), <https://doi.org/10.1021/bi00894a002>.
- [42] H. Dong, C. Unluer, E.-H. Yang, A. Al-Tabbaa, Synthesis of reactive MgO from reject brine via the addition of NH₄OH, *Hydrometallurgy* 169 (2017) 165–172, <https://doi.org/10.1016/j.hydromet.2017.01.010>.
- [43] H. Dong, E.-H. Yang, C. Unluer, F. Jin, A. Al-Tabbaa, Investigation of the properties of MgO recovered from reject brine obtained from desalination plants, *J. Clean. Prod.* 196 (2018) 100–108, <https://doi.org/10.1016/j.jclepro.2018.06.032>.
- [44] M. Turek, W. Gnot, Precipitation of magnesium hydroxide from brine, *Ind. Eng. Chem. Res.* 34 (1995) 244–250, <https://doi.org/10.1021/ie00040a025>.
- [45] E. Alvarado, L.M. Torres-Martinez, A.F. Fuentes, P. Quintana, Preparation and characterization of MgO powders obtained from different magnesium salts and the mineral dolomite, *Polyhedron* (2000) 2345–2351, [https://doi.org/10.1016/S0277-5387\(00\)00570-2](https://doi.org/10.1016/S0277-5387(00)00570-2).
- [46] T.G. Venkatesha, R. Viswanatha, Y. Arthoba Nayaka, B.K. Chethana, Kinetics and thermodynamics of reactive and vat dyes adsorption on MgO nanoparticles, *Chem. Eng. J.* 198–199 (2012) 1–10, <https://doi.org/10.1016/j.cej.2012.05.071>.
- [47] F. Jin, A. Al-Tabbaa, Characterisation of different commercial reactive magnesia, *Adv. Cem. Res.* 26 (2) (2014) 101–113, <https://doi.org/10.1680/adcr.13.00004>.
- [48] A.F. Mohammad, M.H. El-Naas, A.H. Al-Marzouqi, M.I. Suleiman, M. Al Musharfy, Optimization of magnesium recovery from reject brine for reuse in desalination post-treatment, *J. Water Process. Eng.* 31 (2019), 100810, <https://doi.org/10.1016/j.jwpe.2019.100810>.
- [49] O. Lehmann, O. Nir, M. Kuflik, O. Lahav, Recovery of high-purity magnesium solutions from RO brines by adsorption of Mg(OH)₂(s) on Fe₃O₄ micro-particles and magnetic solids separation, *Chem. Eng. J.* 235 (2014) 37–45, <https://doi.org/10.1016/j.cej.2013.09.014>.
- [50] I. Singh, R. Hay, K. Celik, Recovery and direct carbonation of brucite from desalination reject brine for use as a construction material, *Cem. Concr. Res.* 152 (2022), 106673, <https://doi.org/10.1016/j.cemconres.2021.106673>.
- [51] C.G. Kontoyannis, N.V. Vagenas, Calcium carbonate phase analysis using XRD and FT-Raman spectroscopy, *Analyst* 125 (2000) 251–255, <https://doi.org/10.1039/a908609i>.